Journal of Crystal Growth 312 (2010) 2310–2314

Contents lists available at ScienceDirect

Journal of Crystal Growth

journal homepage: www.elsevier.com/locate/jcrysgro

CdTe nanorods formation via nanoparticle self-assembly by thermal chemistry method

X.N. Wang [a,b,*], J. Wang [a], M.J. Zhou [a], H. Wang [b,*], X.D. Xiao [a], Q. Li [a]

[a] Department of Physics, The Chinese University of Hong Kong, Shatin, New Territory, Hong Kong, China
[b] Faculty of Physics and Electronic Technology, Hubei University, Wuhan 430062, China

ARTICLE INFO

Article history:
Received 22 December 2009
Received in revised form
29 March 2010
Accepted 25 May 2010
Communicated by J.M. Redwing
Available online 1 June 2010

Keywords:
A1. Nanostructures
A1. Characterization
A1. Crystal structure
B2. Semiconducting cadmium compounds

ABSTRACT

CdTe nanorods with diameter of ~150 nm and length of ~1 μm are formed via a self-assembly process of CdTe nanoparticles using thermal chemistry method. Individual nanorod is usually composed of nanoparticles stacking along the rod growth direction, and multiple twins are observed both along the rod's growth and radial directions. The effect of the substrate-to-source distance, evaporation temperature and growth pressure on the products morphology is investigated, which reveals the nanoparticle surface energy reduction and the limited quantity of the evaporated species serve as the driving force for the self-assembly process. A "two-orientation" growth model is proposed for the growth pattern.

1. Introduction

As a direct band gap semiconductor with high atomic number and electron density, CdTe has wide applications in photovoltaics, sensors and detectors [1–3]. In particular, it is an excellent light harvester for solar energy applications due to its large optical absorption coefficient and band gap of ~1.5 eV, which matches the preferred absorption range of the solar spectrum [4]. In recent years, it has been found that its low-dimensional nanostructures such as nanoparticles, nanowires and nanorods may have strong quantum confinement effects and improved photoelectric property [5–9], and thus have great potential in serving as functional building blocks for photovoltaic and optoelectronic nanodevices [10,11].

Compared to the versatile methods of the synthesis of CdTe quantum dots [12–16], the preparation of CdTe nanowires and their growth mechanism discussions are rather limited. Several techniques have been used to fabricate CdTe nanowires. For example, template-directed electrodeposition has been used to grow CdTe nanowires, for they can be restricted into the pores of porous anodized aluminum oxide (AAO) template, resulting in one-dimensional (1D) growth [17–19]. Alternatively, CdTe nanorods growth has also been demonstrated using catalytic driven pulsed laser deposition (PLD) technique, in which a selective area epitaxy on sapphire substrate and a catalytically driven vapor–liquid–solid growth mode are found to be critical for the 1D growth [20,21]. In the AAO templating method, the nanowires crystallinity highly depends on the growth temperature, as electrodeposition at room temperature results in amorphous whereas higher temperature always leads to polycrystalline nanowires. Although the PLD method could generate CdTe nanorods with single crystallinity, control over the size and distribution of the catalytic seeds and substrate surface alteration serves as key factors to limit Ostwald ripening of the seeds and prevent the lateral growth, and ensure the 1D growth. As a comparison, self-assembly of CdTe nanoparticles is a simple method to obtain CdTe nanowires both in well-dispersed and aggregated system. In a well-dispersed CdTe nanoparticle system, Tang et al. [22] have found that the nanoparticles can spontaneously organize into nanowires in solution after partial removal of the capping stabilizer of the nanoparticles. The driven force for such nanoparticle self-assembly into nanowires has been attributed to the strong dipole–dipole interaction among CdTe nanocrystals as well as the Van der Waals force and the hydrogen bonding of the ligand molecules [22–24]. Recently, Cao et al. [25] reported that the CdTe nanoparticles percolated on silicon substrate can also self-organize into long nanowires and nanoribbons after hydrothermal treatment. In such an agglomerated system, the nanowires are formed through the linear aggregation of numerous small particles via oriented attachment, and such a self-assembly process is driven by the surface energy reduction. Although this self-assembly was achieved on a solid substrate

* Corresponding author at. Department of Physics, The Chinese University of Hong Kong, Shatin, New Territory, Hong Kong, China.
Tel.: +852 26961191; fax: +852 26035204.
E-mail addresses: xnwang2006@hotmail.com (X.N. Wang), nanoguy@126.com (H. Wang).

0022-0248/$ - see front matter © 2010 Elsevier B.V. All rights reserved.
doi:10.1016/j.jcrysgro.2010.05.032

surface, the initial CdTe nanoparticles were pre-synthesized using wet chemical method in a condensed solution. Up to date, few reports are available for CdTe nanowires or nanorods formation via nanoparticles self-assembly from a gas phase system.

In this work, CdTe nanorods with an average diameter of ~150 nm and length of ~1 μm were prepared via nanoparticles self-assembly from the gas phase using thermal chemistry growth method. An individual nanorod has been found to be composed of zinc blende nanocrystals with multiple twins. These twins share the $\{1\,1\,1\}_{CdTe}$ planes as the mirror planes along both the nanorod longitudinal and radial directions. The effect of the growth parameters on the nanorod formation have been investigated, based on the results which, the growth mechanism that governs the self-assembly process is discussed, and a "two-orientation" growth model has been proposed here for the nanorod formation.

2. Experimental methods

The CdTe nanorods were deposited on ITO substrates by thermal evaporation. The substrate was sequentially cleaned in acetone, alcohol and distilled water using ultrasound for 10 min each, before it was placed in a glass tube with a flat bottom and transferred into an alumina vacuum tube furnace (Φ3.5 cm × 95 cm). High-purity CdTe powder (5 N) was loaded into an alumina crucible placed at the center of the furnace. The glass tube was positioned at the downstream of the furnace with open end oriented to the source material. Before growth, the oven was evacuated to 2×10^{-1} mbar to reduce the amount of the residual oxygen. The furnace temperature was then raised to 700 °C at a rate of 20 °C/min and held for 30 min during the growth. The substrate was located at a temperature zone 350–400 °C. No carrier gas was used during the whole growth process. The sample was cooled down to room temperature after growth, and a yellow–black film could be clearly seen on the substrate.

The morphology and crystallinity of the CdTe nanorods were examined respectively by field-emission scanning electron microscopy (FE-SEM, FEI Quauta 400F) and X-ray diffraction (XRD, Ragiku RU300) using a Cu Kα1 line. More detailed microstructure characterizations and chemical composition analysis were carried out using a transmission electron microscope (TEM, Tecnai 20, FEG) equipped with an energy dispersive X-ray (EDX) spectrometer.

3. Results and discussion

Fig. 1a is a low-magnification SEM image of the as-grown sample on ITO substrate, with rod-like structures on the substrate in a large area. From a higher magnification SEM image (Fig. 1b), a dense layer of nanocrystals with average size of 35 nm can be seen covering the ITO substrate, and the rod-like structures are found to stem out from the dense nanocrystal layer. The nanorods are oriented randomly with an average diameter of ~150 nm and length of ~1 μm. In addition, each nanorod seems to be composed of a number of nanocrystals stacking along the rod growth direction.

XRD taken from the sample is shown in Fig. 2. Besides the diffraction peaks from the ITO film denoted by asterisk, several reflection peaks can be clearly observed at 23.72°, 39.24° and 46.39°, which can be indexed to the (1 1 1), (2 2 0) and (3 1 1) planes of zinc blende (ZB) CdTe (JCPDS file No. 65-880) with the lattice constant of $a=6.48$ Å, respectively. The intense diffraction intensity of the {1 1 1} plane suggests a preferential orientation of the nanocrystals in the CdTe nanorods and/or film beneath the rods. No other impurity is detected in the XRD spectrum.

The detailed microstructure of individual CdTe nanorods was investigated using TEM-related techniques. Fig. 3a shows a low-magnification TEM image taken from a CdTe nanorod, in which obvious interfaces were observed at the crystal boundaries among the nanoparticles without any void formation. In the EDX spectrum taken from the nanorod (Fig. 3b), only Cd and Te signals could be detected with atomic ratio close to 1:1 (the Cu signal is from the TEM grid). The absence of oxygen signal in the EDX suggests little oxidation of the Cd and Te at a growth pressure of $\sim10^{-1}$ mbar. This agrees well with the XRD results.

The orientation relationships among the adjacent individual nanocrystals in the nanorods are investigated using high-resolution TEM (HRTEM). Here, we illustrate the results by taking three adjacent nanocrystal grains (marked as A, B and C in Fig. 3a) as an example. As shown in Fig. 3c and d, all three crystals have ZB

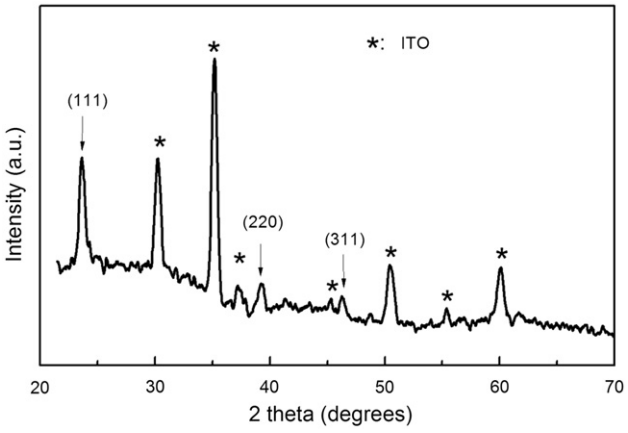

Fig. 2. XRD pattern of the CdTe nanorods on ITO substrate.

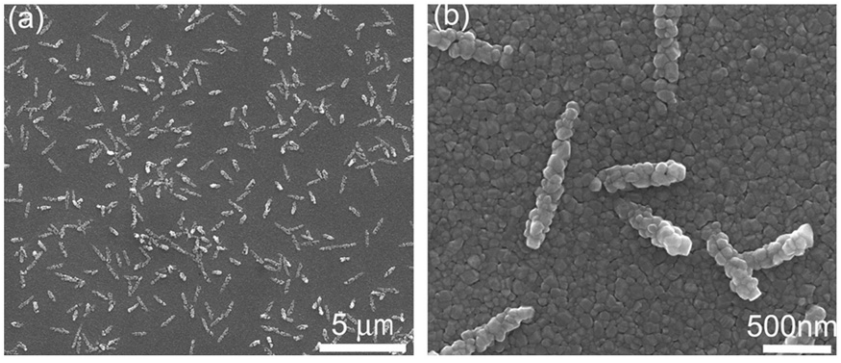

Fig. 1. (a) Low- and (b) high-magnification SEM images of CdTe nanorods on ITO substrate fabricated by thermal chemistry method.

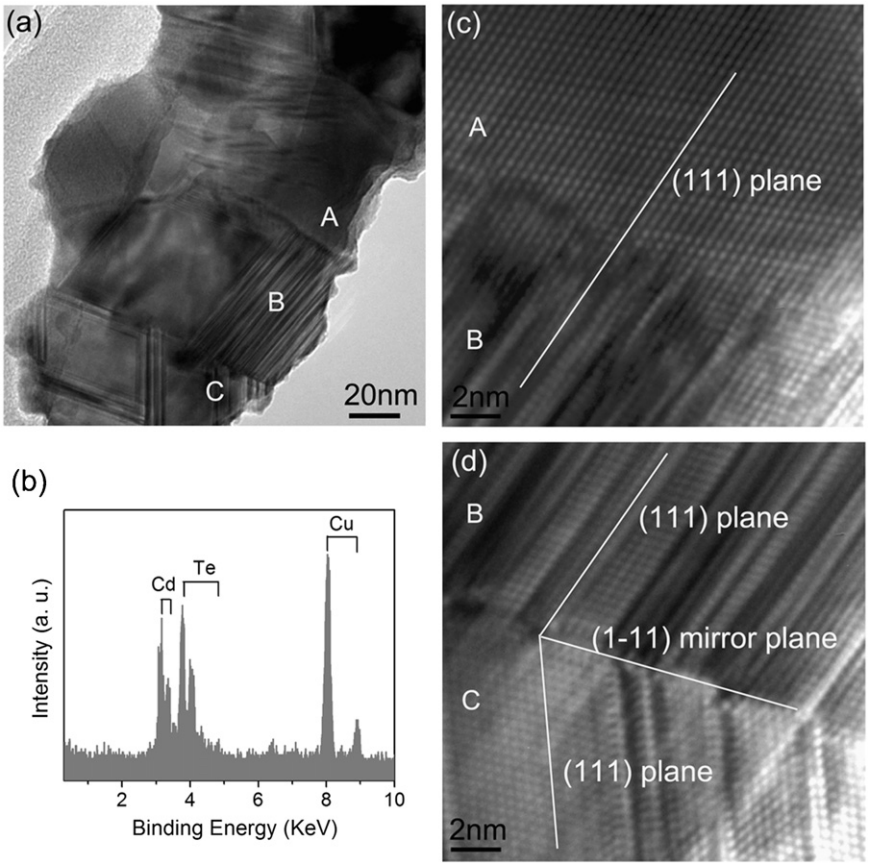

Fig. 3. (a) Low magnification TEM image showing the morphology of single CdTe nanorod; (b) EDX spectrum of the CdTe nanorod shown in (a); and (c) and (d) typical HRTEM images taken from different nanocrystal components in a single CdTe nanorod, when heavy stacking faults could be found in nanocrystals B and C.

structure. Epitaxial relationship was identified between grains A and B, but with only one set of the {1 1 1} planes parallel to each other, i.e., $\{1\,1\,1\}_{\text{A grain}}||\{1\,1\,1\}_{\text{B grain}}$. Heavy stacking faults (SFs) were found in some regions of grain B. The generation of SFs is very likely in CdTe due to their low formation energy as suggested by the *ab initio* calculation [26]. This is similar to the SFs occurred during the growth of CdTe thin films on Si and sapphire substrates [27]. The twin relationship between grains B and C is revealed in Fig. 3d, in which one can find the other set of {1 1 1} plane in nanocrystal B serving as the twin mirror plane.

The CdTe nanorods growth occurs in the absence of any catalyst or substrate modification. Although the melting point of CdTe is up to 1098 °C, its decomposition can occur at a much low temperature in a vacuum system [28]. In the present study, we found decomposition of the CdTe source material occurs at ~700 °C. Considering the low melting temperatures of Te (452 °C) and Cd (321 °C), Cd and Te atoms are expected in vapor phase at 700 °C. Then at the low temperature zone (350–400 °C), Te droplets condense first while most of the Cd remains in vapor phase [29,30]. This would promote the reaction between the Te droplets and Cd vapor to form CdTe nanocrystals.

In order to understand how the CdTe nanorods are formed from the small nanocrystals, the effect of the growth parameters on the morphology of CdTe products have been studied by independently changing several growth parameters, including the distance between substrate and source, the growth pressure and the source evaporation temperature. Four samples B1, B2, B3 and B4 (Table 1) were obtained when single growth parameters were changed from those adopted by the previously discussed sample (denoted as sample A in Table 1), with others being kept the same.

Table 1
CdTe samples prepared by changing one parameter from that used in sample A.

Sample code	Growth pressure (mbar)	Distance from substrate-to-source (cm)	Source temperature (°C)
Sample A	2×10^{-1}	29	700
Sample B1	2×10^{-1}	26	700
Sample B2	2×10^{-2}	29	700
Sample B3	2×10^{-1}	29	730
Sample B4	2×10^{-1}	29	660

Fig. 4a shows the SEM images of sample B1 when the ITO substrate was located at a position close to the source (~26 cm away from the source). It is clear that single crystalline CdTe nanorod arrays with an average diameter of about 100 nm can be formed on the substrate, while the CdTe nanorods composed of nanocrystals assemblies only appear at a position farther away from the source (~29 cm away from the source). In a conventional tube furnace, as the source-to-substrate distance increases, the concentrations of the evaporated species decrease gradually and the growth takes place much slower due to the limited amount of the source material. Hence, for substrate placed closer to the source, the crystal growth will be faster due to the abundant supply of the evaporated atoms in such a region. The observed 1D growth of CdTe is then determined by the fast growth of high energy crystalline planes (anisotropic growth) [31]. At positions father away from the source, the growth process is much slower, which limits the crystal to grow into larger sizes

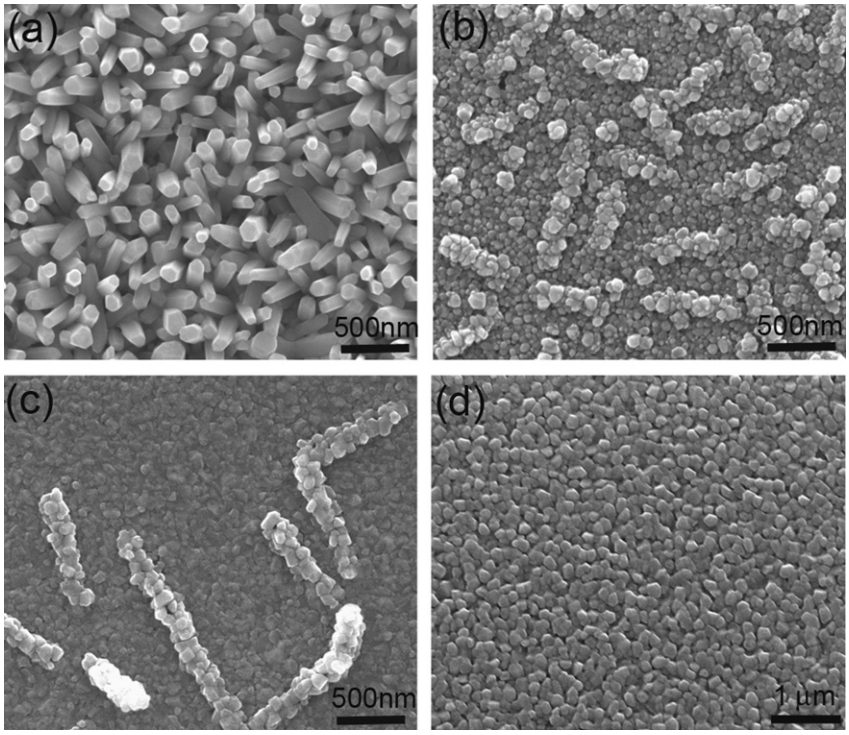

Fig. 4. SEM images of the CdTe samples prepared by changing one of the growth parameters: (a) ITO substrate was located at a position much closer (26 cm) to the source; (b) growth pressure was lowered to 2×10^{-2} mbar; and (c) and (d) evaporation temperature of the source was held at 730 and 660 °C.

[32], although nucleation would still occur as long as supersaturation is reached. This is consistent with the observation of large amount of small-sized nanocrystals and the fact that the CdTe nanorods are composed of nanocrystals in such a region.

The results of samples B2, B3 and B4, in which the concentration of the evaporated atoms (at the same position as sample A) has been tuned by independently changing the growth pressure and source evaporation temperature, also support this hypothesis. Sample B2 was grown at a much lower pressure of 2×10^{-2} mbar (Fig. 4b). In addition to the CdTe nanorods, plenty of larger sized CdTe nanoclusters (with larger size than the nanocrystals that cover the ITO surface) are also observed. Compared to sample A, these CdTe nanorods have a smaller aspect ratio. Since the concentration of the evaporated atoms is inversely proportional to growth pressure, this result suggests that the assembly of nanocrystals into nanorods depends highly on the vapor phase supply. Fig. 4c and d shows samples B3 and B4 that were grown with a source evaporation temperature of 730 and 660 °C, respectively. Similar CdTe nanorods can be found in sample B3 at the same distance and growth pressure (2×10^{-1} mbar) as that of samples A and B1. As a comparison, only CdTe nanocrystal film was formed in sample B4 due to the shortage of the source supply from vapor phase when the source evaporation temperature was decreased to 660 °C. Compared with sample B2, samples A and B3 have better rod-like morphologies with higher aspect ratio and uniformity, which suggests it will benefit the growth of CdTe nanorods at higher growth pressure and source temperature.

For all of the above samples, dense CdTe nanocrystals were formed on ITO surface with the size ranging from 20 to 80 nm. Such nanocrystal layers can serve as a template for the selective growth of CdTe nanorods. Here we propose a "two-orientation" growth model for the self-assembly of the CdTe nanocrystals into nanorods and large sized nanoclusters (illustration schematic can be found in Fig. 5). The CdTe nanorods start from a single CdTe nanocrystal that is formed via reactions of Cd and Te during the thermal evaporation process. Although multiple nucleation is expected, lateral expansion of the nucleated CdTe nanocrystals (further growth) is limited by the shortage in supply of the source from the vapor phase. On the other hand, difference in surface energy of anisotropic crystalline facets makes the {1 1 1} surface of a ZB crystal more active in most of the common cases [32]. As confirmed by the TEM results, the CdTe nanoparticle components have ZB structure. Therefore, the exposed {1 1 1} surfaces of the already nucleated CdTe nanocrystals could further serve as accommodating planes, allowing another CdTe nucleus to attach to it (the assembly process). Such a process would result in reduction in the surface energy of the nanocrystal nuclei. In such a manner, one should expect to see continuous stacking of the nanocrystal nuclei along the CdTe ⟨1 1 1⟩ crystalline direction (the "longitudinal growth" mode), leading to the preferred 1D growth (assembly) into CdTe nanorods, such as samples A and B3.

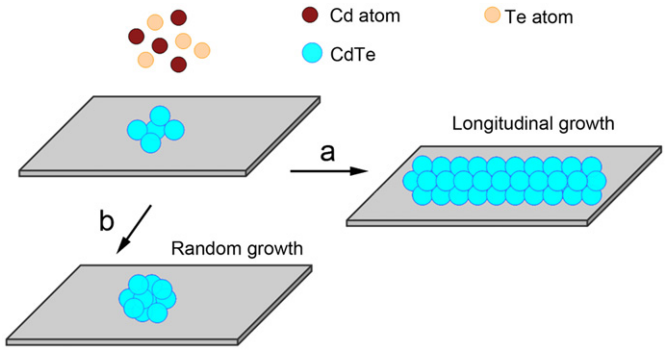

Fig. 5. Schematic illustration of the "two-orientation" growth model for the CdTe nanorods and nanoclusters, which includes the growth of CdTe nanocrystals along longitudinal (indicated by the brown circles) direction (nanorod assembly) and random orientation growth (nanocluster assembly). (For interpretation of the references to colour in this figure legend, the reader is referred to the web version of this article.)

Nevertheless, the nanocrystal nucleus could have more than one {1 1 1} planes as the termination surface, so that side attachment of other nanocrystals is also possible, leading to the lateral expansion of such nanorods. In fact, when such possibility dominates the growth, larger sized CdTe nanoclusters will be easily formed as those found in sample B2, and a "random growth" mode was adopted to describe such a case.

4. Conclusion

In conclusion, CdTe nanorods, with an average diameter of $\sim$150 nm and length of $\sim$1 μm, have been synthesized via the self-assembly of CdTe nanocrystals by a catalyst-free thermal chemistry method. The nanorods were composed of ZB CdTe nanocrystals with a mean diameter of 35 nm by sharing $\{1\ 1\ 1\}_{CdTe}$ planes and/or forming twins along their longitudinal growth direction. Based on the investigation of several growth parameters on the morphology of the final products, the formation mechanism of the CdTe nanorods is understood as driven by the limited concentration of evaporated source and reduction of surface energy.

Acknowledgements

This work is supported by grants from the GRF of HKSAR under project No. 414908, CUHK Group Research Scheme, the National Nature Science Foundation of China (No. 50772032), Research Fund for the Doctoral Program of MOE of China (No. 20060512004), STD and ED of Hubei Province (2008BAB010, Z20091001) and NSF Creative Team Project of Hubei Province (No. 2007ABC005).

References

[1] I. Visoly-Fisher, S.R. Cohen, A. Ruzin, D. Cahen, Adv. Mater. 16 (2004) 879.
[2] N.N. Mamedova, N.A. Kotov, A.L. Rogach, J. Studer, Nano Lett. 1 (2001) 281.
[3] J. Kang, E.I. Parsai, D. Albin, V.G. Karpov, D. Shvydka, Appl. Phys. Lett. 93 (2008) 223507.
[4] A.J. Breeze, The IEEE International Reliability Physics Symposium, Phoenix, 2008.
[5] K.S. Leschkies, R. Divakar, J. Basu, E. Enache-Pommer, J.E. Boercker, C.B. Carter, U.R. Kortshagen, D.J. Norris, E.S. Aydil, Nano Lett. 7 (2007) 1793.
[6] D. Kuang, J. Brillet, P. Chen, M. Takata, S. Uchida, H. Miura, K. Sumioka, S.M. Zakeeruddin, M. Grätzel, ACS Nano 2 (2008) 1113.
[7] B. Tian, X. Zheng, T.J. Kempa, Y. Fang, N. Yu, G. Yu, J. Huang, Nature 449 (2007) 885.
[8] D.V. Talapin, S. Haubold, A.L. Rogach, A. Kornowski, M. Haase, H. Weller, J. Phys. Chem. B 105 (2001) 2260.
[9] X.F. Gao, H.B. Li, W.T. Sun, Q. Chen, F.Q. Tang, L.M. Peng, J. Phys. Chem. C 113 (2009) 7531.
[10] M.H. Huang, S. Mao, H. Feick, Y. Wu, H. Kind, E. Webber, R. Russo, P. Yang, Science 292 (2001) 1897.
[11] P.V.J. Kamat, J. Phys. Chem. C 112 (2008) 18737.
[12] Y. Terai, S. Kuroda, K. Takita, T. Okuno, Y. Masumoto, Appl. Phys. Lett. 73 (1998) 3757.
[13] H. Zhang, L.P. Wang, H.M. Xiong, L.H. Hu, B. Yang, W. Li, Adv. Mater. 15 (2003) 1712.
[14] S.F. Wuister, I. Swart, F. van Driel, S.G. Hickey, C.D. Donegá, Nano Lett. 3 (2003) 503.
[15] T. Rajh, O.I. Micic, A.J. Nozik, J. Phys. Chem. 97 (1993) 11999.
[16] Y. Bae, N. Myung, A.J. Bard, Nano Lett. 4 (2004) 1153.
[17] M.C. Kum, Y.B. Yoo, Y.W. Rheem, K.N. Bozhilov, W. Chen, A. Mulchandani, N.M. Myung, Nanotechnology 19 (2008) 3257111.
[18] A.W. Zhao, G.W. Meng, L.D. Zhang, T. Gao, S.H. Sun, Y.T. Pang, Appl. Phys. A 76 (2003) 537.
[19] D.S. Xu, Y.G. Guo, D.P. Yu, G.L. Guo, Y.Q. Tang, D.P. Yu, J. Mater. Res. 17 (2002) 1711.
[20] S. Neretina, R.A. Hughes, J.F. Britten, N.V. Sochinskii, J.S. Preston, P. Mascher, Nanotechnology 18 (2007) 275301.
[21] S. Neretina, R.A. Hughes, G.A. Devenyi, N.V. Sochinskii, J.S. Preston, P. Mascher, Nanotechnology 19 (2008) 185601.
[22] Z.Y. Tang, N.A. Kotov, M. Giersig, Science 297 (2002) 237.
[23] S. Shanbhag, A.N. Kotov, J. Phys. Chem. B 110 (2006) 12211.
[24] Z. Zhang, Z. Tang, N.A. Kotov, S.C. Glotzer, Nano Lett. 7 (2007) 1670.
[25] X. Cao, X. Lan, Y. Guo, C. Zhao, Cryst. Growth Des. 8 (2008) 575.
[26] Y.F. Yan, M.M. Al-Jassim, T. Demuth, J. Appl. Phys. 90 (2001) 3952.
[27] D.J. Smith, S.-C.Y. Tsen, Y.P. Chen, J.-P. Faurie, S. Sivananthan, Appl. Phys. Lett. 67 (1995) 1591.
[28] E. Bacaksiz, B.M. Basol, M. Altunbaş, V. Novruzov, E. Yanmaz, S. Nezir, Thin Solid Films 515 (2007) 3079.
[29] Q. Wang, G. Chen, N. Zhou, Nanotechnology 20 (2009) 085602.
[30] D.H. Fan, J. Cryst. Growth 311 (2009) 2300.
[31] W.Y. Yin, M.H. Cao, S.J. Luo, C.W. Hu, B.Q. Wei, Cryst. Growth Des. 9 (2009) 2173.
[32] B.A. Wacaser, K.A. Dick, J. Johansson, M.T. Borgström, K. Deppert, L. Samuelson, Adv. Mater. 21 (2009) 153.